



## Exceeding the Betz limit with tidal turbines

Ross Vennell

*Ocean Physics Group, Department of Marine Science, University of Otago, Dunedin 9054, New Zealand*

### ARTICLE INFO

#### Article history:

Received 25 June 2012

Accepted 14 December 2012

Available online 28 January 2013

#### Keywords:

Tidal stream

Resource assessment

Tidal current power

### ABSTRACT

The Betz limit sets a theoretical upper limit for the power production by turbines expressed as a maximum power coefficient of  $16/27$ . While power production by wind turbines falls short of the Betz limit, tidal turbines in a channel can theoretically have a power coefficient several times larger than  $16/27$ . However, power extraction by turbines in large tidal farms also reduces the flow along the channel, limiting their maximum output. Despite this flow reduction, turbines in tidal farms can produce enough power to meet a stricter definition of what it means to exceed the Betz limit, one where the maximum power output of a turbine at the reduced flow exceeds the maximum output from a single Betz turbine operating in the unreduced flow. While having a power coefficient  $>16/27$  is easily achieved by turbines in a channel, generating enough power to meet this stricter definition of exceedance is much more difficult. Whether turbines meet this stricter definition depends on their number, how they are arranged and tuned, and the dynamical balance of the channel. Arranging a tidal turbine farm so that the turbines within it exceed the stricter Betz limit would give tidal turbine farms an economic advantage over similarly sized wind farms. However, exceeding the stricter limit comes at a cost of both higher structural loads on the tidal turbines and the need to produce power from weaker flows. Farms in a channel loosely based on the Pentland Firth are used to discuss exceedance and structural loads.

© 2012 Elsevier Ltd. All rights reserved.

### 1. Introduction

The Betz limit is a theoretical upper limit on the power production from a turbine whose blades sweep a given area [1]. The limit is expressed as a maximum rotor power coefficient of  $C_p = 16/27$ . Wind turbines aspire to achieve this power coefficient, but in practice fall short for several reasons [2]. Many wind and tidal turbine engineers would be surprised by tidal turbines having a power coefficient several times larger than  $16/27$ , because it would indicate that tidal turbines can produce much more power than the theoretical limit. Here it is shown that grouping tidal turbines into large farms in high flow tidal channels makes it relatively easy for the turbines to have  $C_p \gg 16/27$ . However, a large  $C_p$  does not necessarily mean higher power production as power extraction by the farm slows the flow along the channel, reducing the maximum power output of all turbines within the farm ([3], hereafter GC05; [4], hereafter V10). This paper addresses the more complex question, can a turbine in a farm produce more power than a single turbine in the channel operating at the Betz limit? The question is more complex because the turbine in a farm operates in a lower flow than a single turbine on its own in the

channel. In addition, the maximum power production of a turbine in a farm is limited by the degree to which the flow is reduced, which in turn is circularly linked to how much power the turbines collectively extract from the flow, V10. This paper shows that, despite flow reduction, it is still possible for turbines in a farm to exceed the Betz limit of a single isolated turbine, though achieving this is much more difficult than having turbines with  $C_p > 16/27$ .

Tidal turbines exploiting the concentrated energy of high flow channels can make a significant contribution to the demand for renewable energy (see review [5]). To date there are only single 1 Mega Watt (MW) tidal turbines operating [e.g. [6]]. To make a significant contribution to the demand for renewable power tidal turbine farms must scale to a size which can produce 100s of MW. This requires tidal turbine farms with 100s of turbines, a size comparable with large wind farms. On this scale tidal turbine farms in channels may have a significant advantage over similarly sized wind turbine farms. One where the output per turbine is higher than that of a single isolated turbine. Producing more power from each turbine has a strong bearing on the economics of developing tidal current power. This paper is about understanding when it is possible to produce more power from each turbine within a tidal turbine farm than the power produced by a single isolated turbine.

Ref. [7] (hereafter GC07) extended Betz's results to a turbine in a channel. They found that the power coefficient of a turbine in

E-mail address: [ross.vennell@otago.ac.nz](mailto:ross.vennell@otago.ac.nz).

a channel increases as turbines fill the cross-section, i.e. as the turbine blockage ratio increases. This confirms the intuition that turbines in a channel should be more efficient due to the partial duct formed around each turbine due to the proximity of other turbines or the sides of the channel, Fig. 1. However, they also showed that turbine efficiency at converting power lost by the flow into power available for electricity production declines from  $2/3$  to  $1/3$  as the blockage ratio increases. Their first conclusion would suggest that turbines in a tidal channel will always exceed the Betz limit for power production. Their second conclusion indicates that the turbines become less efficient, which seems at odds with the first. However, their conclusions do not apply to turbines in a tidal channel because GC07's tuning of the turbines to maximize output did not allow for the reduction in free-stream flow due to the increased drag which results from power extraction, V10. Laboratory and some numerical models of tidal turbines which demonstrate  $C_p > 16/27$  also do not allow for the effects of free-stream flow reduction in tuning the turbines (e.g. [8,9]). V10 and [10] showed that allowing for the effect of power extraction on the free-stream flow requires tidal turbines to be tuned for a particular channel and turbine arrangement in order to maximize farm output. Increasing the blockage ratio with optimally tuned turbines may deliver more or less power per turbine and the turbines may become more or less efficient than the first turbine installed in the channel [11,12]. Consequently, exceeding the Betz limit, in the sense of producing more power from each tidal turbine is much more complex than GC07's model results, laboratory models and some numerical models which demonstrate  $C_p > 16/27$  would suggest.

Simplistically exceeding the Betz limit means the turbine has a rotor power coefficient  $C_p > 16/27$ . However, this only means that at a given flow velocity a turbine produces more power than a turbine operating at the Betz limit in the same flow velocity. For tidal turbines in a channel free-stream flow reduction limits the maximum power of the turbines. Consequently, a stricter definition for exceeding the Betz limit than  $C_p > 16/27$  is needed. This stricter definition is simply that a turbine operating at the reduced maximum flow produces more power than a single isolated Betz turbine operating in the maximum flow along the channel before any turbines are installed. For channels much wider than a single turbine this stricter definition for exceeding the Betz limit is almost the same as having turbines produce more power than the first turbine installed in the channel. Turbines in a farm which produce more than a single turbine acting alone has important consequences for the economics of farm development.

## 2. Background

Conceptually, an isolated turbine produces power by retarding the flow which passes through it. Retarding the flow causes a wake behind the turbine which widens and eventually mixes with the flow which has passed around the turbine. In Fig. 1  $u$  is the free-stream velocity,  $u_1$  is the velocity through the turbine,  $u_3$  is the

velocity in the wake downstream of the turbine and  $u_4$  is the velocity of the flow passing around the turbine. Further downstream of the turbine, shear induced turbulent mixing homogenizes the flow across the channel. If the force exerted by a turbine on the flow is  $F$ , then the power available for electricity production is simply

$$P = Fu_1 \quad (1)$$

The turbine drag force  $F$  and the turbine power  $P$  can be parameterized in terms of the oscillating free-stream tidal velocity by

$$F = \frac{1}{2}\rho C_T A_T |u|u \quad P = \frac{1}{2}\rho C_P A_T |u|^3 \quad (2)$$

where  $C_T$  is the drag coefficient of a single turbine,  $A_T$  is the area swept by the turbine's blades,  $\rho$  the water density and  $C_P$  is the power coefficient. The two coefficients are related by  $C_P = r_1 C_T$ , where  $r_1 = u_1/u$  is the velocity through the turbine relative to the free-stream velocity.  $r_1$  is also the efficiency of the turbine at converting power lost by the flow into power available for electricity generation [13]. The classic measure of turbine efficiency,  $C_p$ , is the ratio of power produced by the turbine to the rate at which Kinetic Energy would flow through the area swept by the turbine's blades in the free-stream flow.

### 2.1. The Betz limit

For a single turbine in an infinite ocean, classic Lanchester–Betz theory can be used to derive an expression for the force exerted by the turbine [14,1]. This is done by using mass continuity, applying Bernoulli's principle upstream and downstream of the turbine and considering momentum fluxes in and out of a control volume surrounding the turbine, in Fig. 1, with  $u_4 = u$  [2]. One result is that the velocity through the turbine must be the average of the velocities upstream and downstream of the turbine, i.e.  $u_1 = (1/2)(u + u_3)$  or

$$r_1 = \frac{1}{2}(1 + r_3) \quad (3)$$

where  $r_3 = u_3/u$ . The force on the turbine is  $F = (1/2)\rho A_T (u^2 - u_3^2)$ , so that for an isolated turbine

$$C_T = 1 - r_3^2 \quad (4)$$

and the power produced (1) is  $P = (1/4)\rho A_T (u - u_3)(u + u_3)^2$ , so that

$$C_P = \frac{P}{\frac{1}{2}\rho A_T |u|^3} = \frac{1}{2}(1 - r_3)(1 + r_3)^2 \quad (5)$$

though traditionally these expressions are written in terms of axial induction factors such as  $a = 1 - r_3$ .

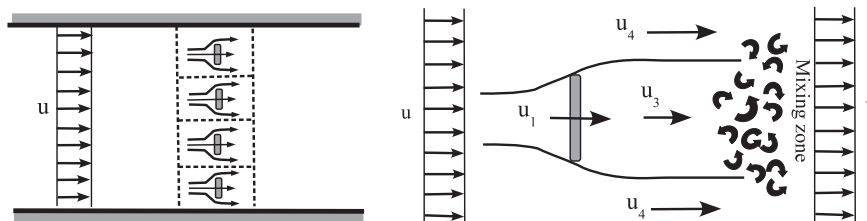


Fig. 1. Schematic of a row of turbines in a tidal channel and the velocities around a single turbine. The velocities are such that  $|u_4| \geq |u| \geq |u_1| \geq |u_3|$ , where  $u$  is the oscillating free-stream tidal velocity upstream and downstream of a row of turbines.

For a single turbine in an infinite flow the free-stream velocity will not be affected by the drag due to power extraction. Thus maximizing the power from the turbine can simply be achieved by maximizing  $C_p$  in equation (5), which requires  $r_3$  to be tuned to a value of  $1/3$ . Consequently, for an isolated turbine the maximum power output is given by the power coefficient  $C_p = 16/27$ , for which the drag coefficient  $C_T = 8/9$  and  $r_1 = 2/3$ . Isolated turbines without ducting cannot exceed this power coefficient, which sets the theoretical upper limit for turbine power production. Wind turbines fall short of the Betz limit power coefficient for several reasons, for example due to the energy lost to creating rotational motion in the turbine's wake and to aerodynamic drag forces on the turbine blades [2]. A single turbine in a tidal channel much wider than the size of the turbine will also be subject to the Betz limit of  $C_p = 16/27$  and will fall short of the limit for many of the same reasons.

## 2.2. Turbines in a channel: GC07

GC07 extended classic turbine theory to a turbine in a narrow channel at low Froude number, generalizing the expressions in the previous section for a Betz turbine, Fig. 1. From their results Equation (3) becomes

$$r_1 = \frac{r_3(r_4 + r_3)}{r_4 + 2r_3 - 1} \quad (6)$$

where  $r_4 = \left(1 - r_3 + \sqrt{\varepsilon - 2\varepsilon r_3 + (1 - \varepsilon + \varepsilon^2)r_3^2}\right)/(1 - \varepsilon)$ . Within this  $\varepsilon = MA_T/A_c$  is the turbine blockage ratio of the channel, where  $M$  is the number of turbines in a row spanning the channel and  $A_c$  is the cross-sectional area of the channel. The turbine blockage ratio will be limited by the need to maintain navigation along the channel. The drag coefficient (4) becomes

$$C_T = r_4^2 - r_3^2 \quad (7)$$

and the power coefficient (5) generalizes to

$$C_p = \frac{r_3(r_4 + r_3)(r_4^2 - r_3^2)}{r_4 + 2r_3 - 1} \quad (8)$$

Surprisingly, GC07 found that this power coefficient was also maximized by  $r_3 = 1/3$ , the same value as the isolated Betz turbine. They showed that for  $r_3 = 1/3$ , and at higher  $\varepsilon$  values, the power coefficient was increased by a factor of  $1/(1 - \varepsilon)^2$  above the Betz value of  $16/27$ , thus exceeding the Betz limit is a simple consequence of adding turbines to a row, which increases  $\varepsilon$ . A second conclusion was that the fraction of the power lost by the flow which is available for power production is  $2/(3(1 + \varepsilon))$ , with the remaining fraction dissipated as heat by mixing behind the turbine ([13]; GC07). Thus the efficiency of converting power lost by the flow into power available for electricity production declines from  $2/3$  to  $1/3$  as turbines fill the cross-section.

GC07's approach to maximizing the power assumes that the free-stream is fixed. However, this does not apply to tidal channels, as power extraction reduces the free-stream flow, GC05. Thus their conclusions about increasing power coefficient and decreasing conversion efficiency do not apply to turbines in tidal channels. For turbines in tidal channels a more sophisticated optimization of the power is required, V10.

## 2.3. Optimal tuning: V10

In short narrow channels, which typically have the high flows required for tidal turbine farms, the free-stream flow is not fixed

but changes due the drag on the flow which results from power extraction. GC05 give a model for a turbine farm in a short [15,16] narrow channel driven by an oscillating head loss between its ends. The channel connects two large water bodies which are so large that power extraction in the channel has no effect on water levels within them. V10 gives an approximate analytic solution to GC05's model, which for a channel with a uniform rectangular cross-section, can be written as [11]

$$u_{\max} = \frac{\sqrt{2}u_1}{\sqrt{\sqrt{4\lambda_{\text{Total}}^2 + 1} + 1}} \quad (9)$$

where the free-stream flow is  $u = u_{\max}\sin(\omega t)$ ,  $\lambda_{\text{Total}} = \alpha(LC_D/h + \varepsilon N_R C_T/2)$  is a rescaled total drag coefficient due to the combined effects of bottom friction and power extraction. Within this,  $L$  is the channel length,  $h$  is the channel depth,  $C_D$  is the bottom drag coefficient and  $N_R$  is the number of rows of turbines in the farm.  $\alpha = 8g\Delta/3\pi\omega^2 L^2$ , where  $\omega$  is the angular frequency of the tide and  $\Delta$  is the amplitude of the water level difference between the ends of the channel. The velocity scale  $u_1 = g\Delta/\omega L$ , is the velocity along the channel when there is no drag. Increasing  $C_T$ , adding turbines to the cross-section or adding rows increases  $\lambda_{\text{Total}}$ , which from Equation (9) decreases the free-stream velocity everywhere along a short narrow channel.

To maximize farm output when power extraction changes the free-stream flow requires the product  $C_p u_{\max}^3$  to be maximized, as  $C_p$  (8),  $u_{\max}$  (9) and  $C_T$  (7) all depend on  $r_3$ , V10. This optimization is done by numerically adjusting or tuning  $r_3$  to maximize the farm's average output over a tidal cycle. However, for a simple sinusoidal tidal velocity the average output of the farm is just  $4N_R M/3\pi$  times the maximum output of a single turbine. As a result the optimal tuning,  $r_3^{\text{opt}}$ , which maximizes the output of the farm of a fixed size and arrangement, also maximizes the output of the turbines within it.

The optimal tuning,  $r_3^{\text{opt}}$  depends on the dimensions of the particular channel, its dynamical balance and how the farm is arranged (V10; [10]). Maximizing the output of turbines within a farm requires a different value of  $r_3$  than that needed to maximize the output of an isolated turbine and thus,  $C_p$  at maximum output for a turbine in a farm differs from the  $16/27$  of an isolated turbine.

For this work a stricter definition of exceeding the Betz limit is required, one based on the power production from a Betz turbine operating in the velocity  $u_0$ , the maximum flow in the channel before any turbines are installed, which is given by  $P_{\text{Betz}} = 0.5(16/27)\rho A_T u_0^3$ . This stricter definition of exceeding the Betz limit requires

$$C_p u_{\max}^3 > \frac{16}{27} u_0^3 \quad (10)$$

The two cases of  $C_p$  which are of interest are V10's optimal tuning  $C_p^{\text{opt}} = C_p(r_3^{\text{opt}}, \varepsilon)$ , which maximizes farm and turbine output, and GC07's tuning for a fixed free-stream flow  $C_p^{1/3} = C_p(1/3, \varepsilon)$ .

## 2.4. Pentland Firth, UK

The strong tidal currents through the Pentland Firth to the south of the Orkney Islands have a considerable potential for tidal current power generation [17]. An example channel loosely based on the Firth is used to present numerical results in Sections 3–6 of this paper, Table 1. The Firth is around 23 km long and varies in depth from 60 to 100 m along its main axis. Its width varies considerably, with 7.5 km being taken as representative of the width of the region

**Table 1**

An example of a short tidal channel loosely based on the Pentland Firth. Tides are based on an average tide using the amplitude and phases of the M2 tide at the ends of the Firth,  $\rho = 1025 \text{ kg m}^{-3}$  and  $C_D = 0.005$  [18]. Power available values are an upper bound at peak flow, they do not include the effects of losses due to turbine support structure, nor electro-mechanical losses, power conversion or transmission losses. Turbine numbers are approximate and based on a turbine with a blade area of  $400 \text{ m}^2$ .

Length, $L$	23 km
Depth, $h$	70 m
Width, $W$	7.5 km
Cross-sectional area, $A$	$0.53 \text{ km}^2$
Peak tidal flow without turbines, $u_0$	$2.5 \text{ m s}^{-1}$
Head loss amplitude, $\Delta$	1.2 m
$u_t$	$3.7 \text{ m s}^{-1}$
$\alpha = u_t/\omega L$	1.0
$\lambda_0 = \alpha L C_D/h$	1.6
Power from turbine at Betz limit at peak tidal flow $u_0$	1.9 MW
$C_p/C_T$ , i.e. $(16/27)/(8/9)$	0.59/0.89
Average tidal current potential	3100 WW
Maximum output at peak tidal flow	7400 MW
Peak tidal velocity at maximum output, $u_{\max}$	$1.4 \text{ m s}^{-1}$
Farm with 680 optimal tuned turbines in 3 rows and $\varepsilon = 0.2$ at peak tidal flow	
Power available per turbine	2.3 MW
$C_p^{\text{opt}}/C_T^{\text{opt}}$	0.91/1.5
Peak tidal flow, $u_{\max}$	$2.3 \text{ m s}^{-1}$
Flow reduction ratios $r_1/r_3$	0.62/0.40
Power available from farm	1800 MW

of high flow along the Firth. Maximum flows can exceed  $4.5 \text{ m s}^{-1}$  in some locations within the Firth at spring tides. In the example, the amplitudes and tidal phases of the M2 tide at the ends of the Firth from the 2D model of Ref. [18], which were based on Topex-Poseidon satellite data validated by coastal tide gauges [19], were used as boundary condition to V10's short channel model (9). These gave  $u_0 = 2.5 \text{ m s}^{-1}$  as representative of the cross-sectional average velocity for an average tide, though the Firth has much stronger flows near the surface in its narrowest cross-section at spring tides. For the loosely based example the potential is 3100 MW averaged over a tidal cycle and 7400 MW at the peak in M2 tidal flow. The rough bottom of the Firth gives a high bottom drag coefficient estimated at  $C_D = 0.005$  [18], which is double the normal value. This is justified in Ref. [18] as being associated with a bed roughness of 0.375 m, which loosely corresponds to 90% of grain sizes being less than 0.2 m. This may be reasonable given that parts of the bottom of the Firth are covered with rocks. Dynamically the Firth has  $\lambda_0 = \alpha L C_D/h \approx 1.6$ , so that bottom friction is of moderate importance in its dynamical balance, V10. The Firth has a similar dynamical balance to the smaller Kaipara Harbour channel NZ, which has weaker flows  $u_0 = 1.7 \text{ m s}^{-1}$  and  $\lambda_0 = 1.5$  [20]. The importance of bottom friction to the Firth can also be seen in  $u_t = 3.7 \text{ m s}^{-1}$ , which is the velocity in the Firth if there were no drag, in comparison to the much smaller  $u_0 = 2.5 \text{ m s}^{-1}$  given by Equation (9) when there is only bottom drag, Table 1.

The turbine numbers presented here are based on turbines with a  $400 \text{ m}^2$  blade area, for which an isolated Betz turbine produces 1.9 MW at the  $2.5 \text{ m s}^{-1}$  peak flow in the undisturbed example channel, Table 1. The largest commercially operating turbine has a similar blade area and an 89% overall efficiency. It also has its power output capped at 1.2 MW at  $2.25 \text{ m s}^{-1}$  to limit structural loads and requires a minimum of  $0.7 \text{ m s}^{-1}$  to produce power [6]. None of these speed restrictions have been incorporated in the results presented here, neither has the overall efficiency due to losses in the turbine's power train, power conversion or electrical transmission.

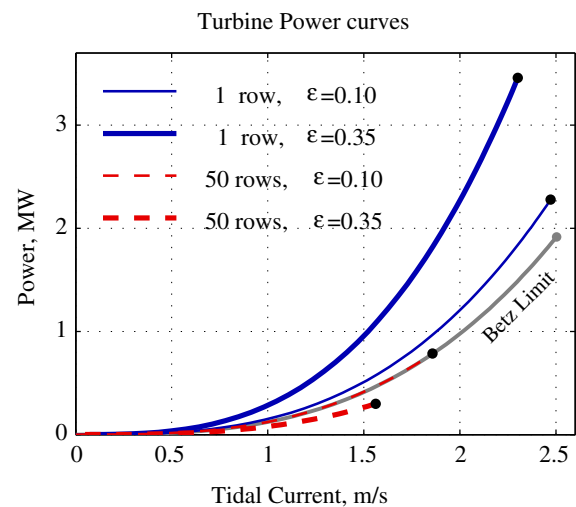
### 3. Power curves for a turbine in a farm

Fig. 2 shows power curves for turbines tuned to maximize farm output in relation to a turbine at the Betz limit, i.e. in relation to the first turbine installed in the channel. For a single row with  $\varepsilon = 0.1$  the power curve rises more rapidly than a turbine at the Betz limit because the power coefficient  $C_p^{\text{opt}} = 0.73 > (16/27) = 0.59$ . Increasing the channel blockage ratio to  $\varepsilon = 0.35$  allows turbines to deliver 35% more power due to increasing the power coefficient to  $C_p^{\text{opt}} = 1.4$ . However, the reduction in maximum flow means that the maximum power output is less than would be expected from more than doubling the power coefficient of an isolated Betz turbine. For a very large 50 row farm with  $\varepsilon = 0.1$  the power curve for the turbines lies over that of the Betz turbine, i.e.  $C_p^{\text{opt}} \approx 16/27$ , though the maximum output is much lower due to a significant reduction in peak flow. For a 50 row farm  $\varepsilon = 0.35$  the power curve lies below the Betz turbine as  $C_p^{\text{opt}} < 16/27$  and maximum output is even more limited by peak flow reduction. This raises the question, why not just decrease  $r_3$  to increase  $C_p$  to  $16/27$ ? Doing so would lift the  $\varepsilon = 0.35$  power curve up to overlap the Betz curve, however it would also reduce the maximum flow so that the maximum output of the turbine is below that of the turbine with  $C_p^{\text{opt}} < 16/27$ . Consequently, for very large farms  $C_p^{\text{opt}}$  may fall below the Betz limit of  $16/27$  in order to maximize turbine and farm output.

Fig. 2 demonstrates that the power curves for a turbine in a farm are not the same as the curve of an isolated Betz turbine. The power curves in a farm may lie above or below the Betz curve and their maximum power output will be limited by reduction in peak flow due to power extraction by the farm. Fig. 2 demonstrates that  $C_p^{\text{opt}}$  and maximum output may increase or decrease with blockage ratio  $\varepsilon$ , but  $C_p^{\text{opt}}$  appears to decrease as rows are added to the farm.

### 4. Optimal $C_T$ and $C_p$ for a turbine in a farm

Fig. 3a) gives the power coefficient at maximum turbine output  $C_p^{\text{opt}}$  as optimally tuned turbines fill a single row, increasing the blockage ratio in the example channel. For a highly blocked channel,  $C_p^{\text{opt}}$  can be eight times that of a Betz turbine. This does not



**Fig. 2.** Power curves for optimally tuned turbines in a 1 row farm or a 50 row farm with channel blockage ratios of  $\varepsilon = 0.1$  or  $0.35$ . The farm is sited in a channel loosely based on the Pentland Firth, Table 1. Thick gray line is the power curve for an isolated Betz turbine  $P = 0.5(16/27)\rho A_T |u|^3$  operating in the flow the channel has before any turbines are installed. Solid dots show power available at peak tidal flow, demonstrating the reduction in peak flow due to power extraction by the turbines. (For interpretation of the references to color in this figure legend, the reader is referred to the web version of this article.)

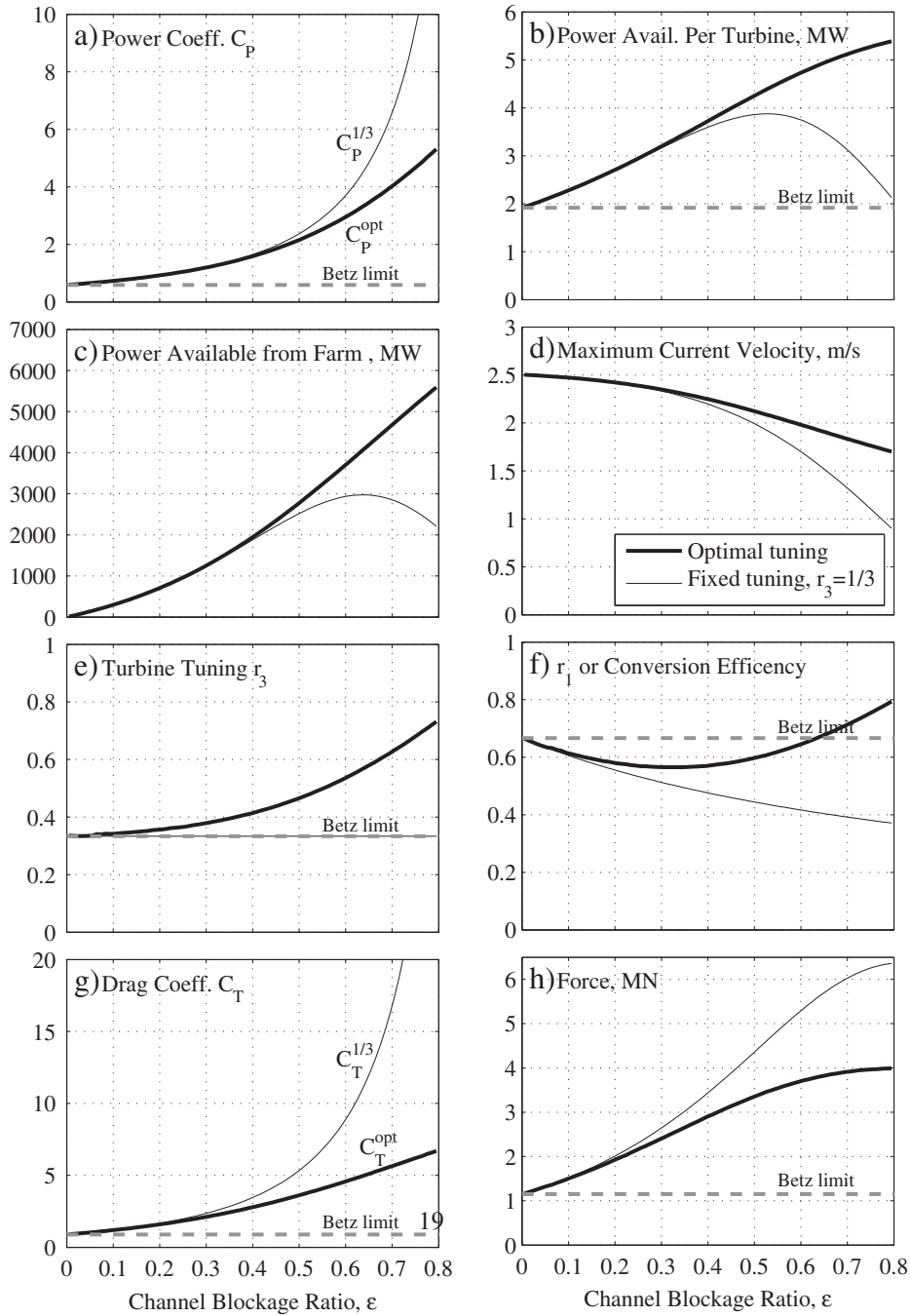


**Fig. 3.** Effect of increasing channel blockage ratio on the turbines and farm at peak flow. Farm has a single row of turbines and is sited in channel loosely based on the Pentland Firth. Gray horizontal dashed line is the value in each plot at the Betz limit, i.e. for a lone Betz turbine. The upper right plot shows that all farms in this figure meet the stricter definition of exceeding the Betz limit (10) as the power per turbine is higher than a lone Betz turbine.

translate into eight times the power, as flow reduction limits power production per turbine to around 2.5 times that of a Betz turbine, Fig. 3b). The power coefficient at the fixed tuning  $r_3 = 1/3$  found by GC07,  $C_p^{1/3}$  shown by the thin line in Fig. 3a), is even larger than  $C_p^{opt}$ , but this translates into less power per turbine than optimal tuning, as a fixed tuning has a greater flow reduction, Fig. 3d). Adopting the fixed tuning  $r_3 = 1/3$  also results in lower farm output in Fig. 3c), with both farm output and the power per turbine declining at high blockage ratios, whereas both increase for optimal tuning. Fig. 3e) shows how optimal tuning increases with blockage ratio. Interestingly the efficiency at converting power lost by the flow into power available for production  $r_1$  in Fig. 3f) mostly falls below that

of the first turbine installed, but is better than the efficiency  $r_1$  at a fixed tuning. Consequently, optimally tuned turbines have less flow reduction behind the turbines, i.e. higher  $r_3$  and  $r_1$ , which results in lower forces on the turbines, Fig. 3h).

What is not obvious in Fig. 3 is that power production from an optimally tuned turbine increases despite a weaker flow reduction in the turbine's wake, i.e. a higher  $r_3$ . It is possible to get more power from a turbine with less flow reduction in the wake because the energy source progressively changes from momentum loss by the flow, to head loss across the farm, as the blockage ratio increases [11]. This higher turbine output comes at a cost of higher structural loads on the turbine's blades and support structure,

Fig. 3h), despite the weaker maximum free-stream flow  $u_{max}$ . Interestingly, the loads on an optimally tuned turbine are lower than those on turbine with a fixed tuning. While  $C_p^{opt}$  and  $C_p^{1/3}$  are similar for a single row with blockage up to  $\epsilon = 0.4$ , the loads on turbines with a fixed tuning rise above those on optimally tuned turbines at a lower blockage ratio of  $\epsilon = 0.25$ . Thus at lower blockage ratios optimal tuning is more important for keeping structural loads down than producing more power.

Fig. 4b) shows how both  $C_p^{opt}$  and the power per turbine diminish as rows are added to a farm, with a greater rate of decline at the higher blockage ratio. Turbines in a single row farm

with a modest blockage ratio of  $\epsilon = 0.1$  produce 19% more power than the first turbine installed, while  $\epsilon = 0.3$  produces 80% more, Fig. 4b). For both blockage ratios all farms shown have  $C_p^{opt} > 16/27$ , but farms with less than 6–8 rows also meet the stricter definition of exceeding the Betz limit (10) with a power per turbine greater than that from the first turbine. Fig. 4c) demonstrates a diminishing return on additional rows [12], though adding rows reduces both the drag coefficient and load on the turbines, Fig. 4g) and h). Adding rows also results in less flow reduction behind the turbines, i.e. higher  $r_3$  in Fig. 4e), and higher conversion efficiency  $r_1$ , Fig. 4f).

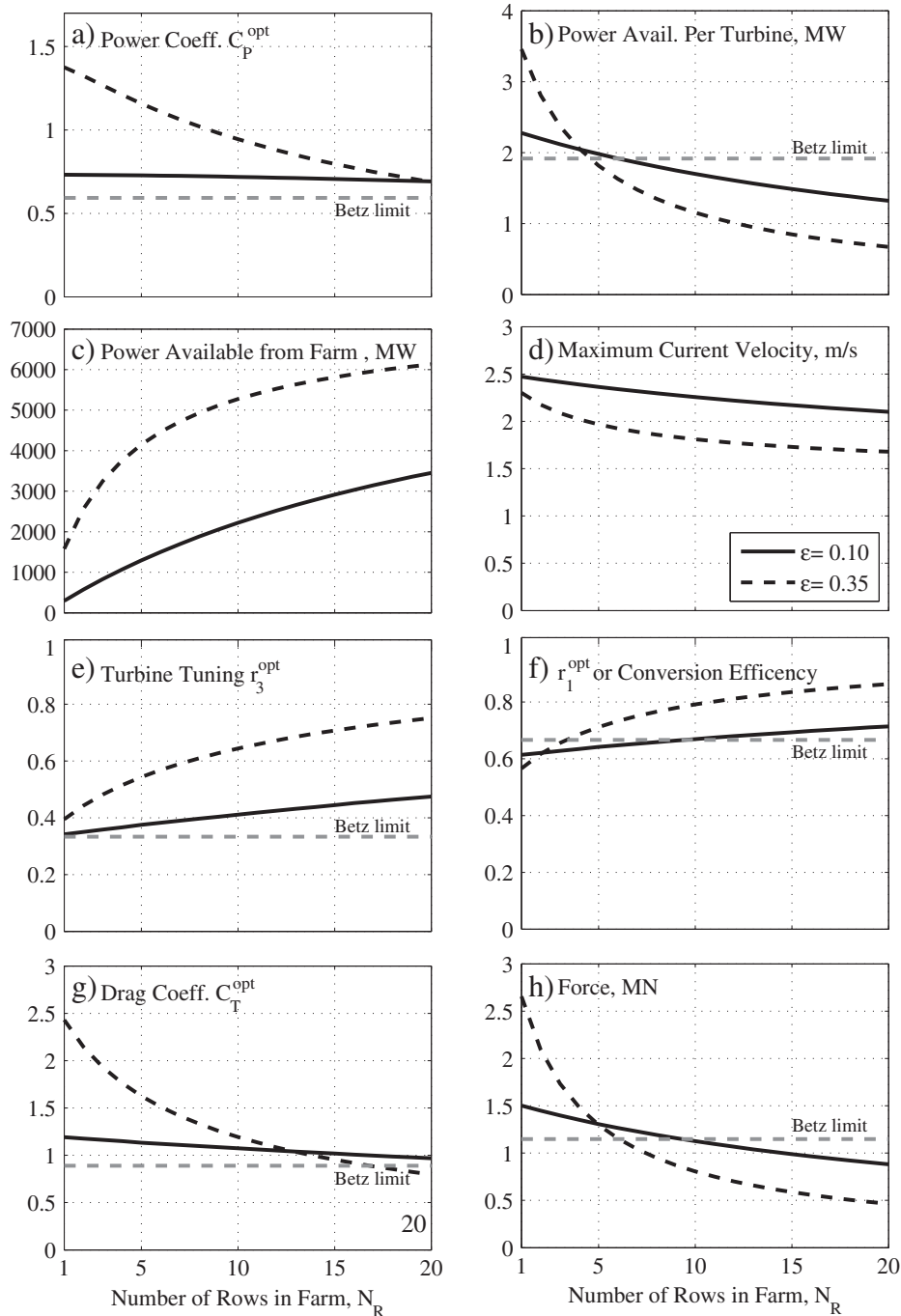


Fig. 4. Effect of increasing the number of rows in a farm with blockage ratios,  $\epsilon = 0.1$  and  $0.35$ , at peak tidal flow. Farm is sited in channel loosely based on the Pentland Firth. Gray horizontal dashed line is the value in each plot at the Betz limit, i.e. for a lone Betz turbine. The upper right plot shows that farms with less than 6–8 rows meet the stricter definition of exceeding the Betz limit (10), with a power output per turbine greater than a lone Betz turbine.

Nishino and Willden [9] developed a 3D CFD model of a tidal turbine which used a novel blade-induced turbulence model. They explored the effect of channel blockage on power and drag coefficients. They assumed the free-stream flow was fixed and tuned the turbine for each value of  $\epsilon$ . Thus conceptually their farm model is closer to GC07's fixed free-stream flow optimization. At their lowest blockage, equivalent to  $\epsilon = 0.03$  their optimal  $C_p = 0.6$ , lay close to the Betz limit. At their highest blockage ratio  $\epsilon = 0.50$  their optimal  $C_p = 2.4$ , close to the  $C_p^{1/3}$  values for a single row in Fig. 3a), while  $C_p^{\text{opt}} = 2.2$  is slightly smaller. Nishino and Willden's [9] blockage ratio of  $\epsilon = 0.35$  gives  $C_p = 1.4$ , almost the same value as the single row farm in Fig. 4a) at  $\epsilon = 0.35$ . However, adding rows quickly reduces  $C_p$  below this value, as significant power extraction slows the free-stream flow, Fig. 4d). Nishino and Willden's [9] optimal drag coefficient for  $\epsilon = 0.50$  is around  $C_T = 5.7$ , similar to the  $C_T^{1/3} = 5.5$  at this blockage ratio in Fig. 3g), however optimally tuned turbines have a lower  $C_T^{\text{opt}} = 3.7$ . Thus the fixed free-stream flow results of Ref. [9] produce similar power to an optimally tuned single row up to  $\epsilon = 0.50$ , however the loads on the optimally tuned row are much lower. At higher  $\epsilon$ , or as more rows are added, the advantage of optimal tuning over a fix free-stream flow tuning, to both power production and structural loads, increases. Consequently, Nishino and Willden's [9] fixed free-stream flow results are restricted to small single row farms which only extract a small fraction of a channel's potential to produce power.

An increasing blockage ratio also increases the velocity between the turbines,  $u_4$ , which may create Froude numbers which are not small as assumed in GC07's results (6)–(8). In Fig. 3  $\epsilon$  ranges between  $\epsilon = 0.0$ – $0.8$  and the free-stream Froude number in the example channel varies from 0.096 to 0.070, so remains small. The reduction in free-stream flows at higher  $\epsilon$  assists to keep Froude numbers around the turbine small. For optimally tuned turbines at the highest blockage ratio in Fig. 3  $u_4 = 4.6 \text{ m s}^{-1}$  and the Froude number is 0.17, which is small enough to justify using GC07's results. A fixed tuning has a higher maximum velocity  $u_4 = 5.7 \text{ m s}^{-1}$ , for which the Froude number is 0.21.

McAdam et al. [21] presented power coefficients for an experimental horizontal axis tidal turbine for blockage ratios up to 0.625 in a flume. They tuned their turbine by changing blade pitch. Their results are comparable to GC07's fixed free-stream flow model, or more precisely, their high depth blockage ratio results are comparable to Houlby et al.'s [22] generalization of GC07's model to include free surface effects [23]. Their  $C_p$  varied with Froude number, but their mid-range results had  $C_p = 0.6$  and 1.3 for blockage ratios of  $\epsilon = 0.5$  and 0.65 respectively. However, comparing with GC07's peak power coefficients is not particularly useful as the high depth blockage ratio of the horizontal axis model turbine needs to be compared to Ref. [22]. Here it is only important to note that there are experimental results which exceed the Betz limit for an isolated turbine.

## 5. Meeting the stricter definition of exceeding the Betz limit

Fig. 5 shows that many farm configurations have  $C_p^{\text{opt}} > 16/27$ . A few very large farms have  $C_p^{\text{opt}} < 16/27$ . What is not shown in the figure is that the power from the farm increases slowly for farms with more than 10 rows due to a harsh diminishing return on additional rows. Thus all sensibly sized farms have  $C_p^{\text{opt}} > 16/27$ . The light blue area in Fig. 5 demonstrates that only relatively small farms can meet the stricter definition of exceeding the Betz limit (10).

Fig. 6 gives more detail, showing that to significantly exceed the stricter definition of the Betz limit (10) a farm in the example channel must have fewer than 3 rows and  $\epsilon > 0.25$ . These small farms have turbines producing  $>2.4 \text{ MW}$ , much higher than the

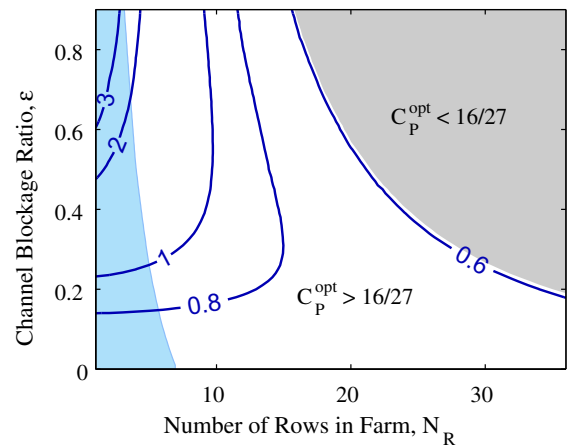


Fig. 5. Contours of  $C_p^{\text{opt}}$  in the example channel for a range of farm configurations. Configurations in gray area have  $C_p^{\text{opt}} < 16/27$  and those in white area have  $C_p^{\text{opt}} > 16/27$ . Light blue area has  $C_p^{\text{opt}} > 16/27$  and also meets the stricter definition of exceeding the Betz limit (10). Note  $C_p^{1/3} \geq 16/27$  for all configurations. (For interpretation of the references to color in this figure legend, the reader is referred to the web version of this article.)

1.9 MW from an isolated Betz turbine. These smaller farms also have less total power available from the farm. Consequently, to take advantage of the stricter definition for exceedance it is necessary to accept a lower total output from the farm. Consequently the size and arrangement of a farm with turbines which meet the stricter definition of exceedance is a compromise between maximizing power output of each turbine and maximizing the total output of the farm. This makes meeting the stricter definition much more difficult than having turbines with  $C_p^{\text{opt}} > 16/27$ .

The dashed black line in Fig. 6 divides configurations which meet the stricter definition (10) in two. Those on the left of the line have an additional benefit, where adding turbines to the rows increases the output of all turbines in the farm, as demonstrated by increasing values of the green power per turbine contours as  $\epsilon$  increases. Thus these configurations also have an increasing return on turbines added to the rows [11].

Fig. 6 also shows that, in the Pentland-like example channel, three rows of optimally tuned turbines with a blockage ratio of  $\epsilon = 0.2$  could make around 1800 MW of power available from the farm at peak flow. This would require 680 400  $\text{m}^2$  turbines, Table 1, with each making 2.3 MW available, i.e. around 0.4 MW more than an isolated turbine at the Betz limit. This number of turbines and blade area is based on the largest commercially operating turbine. However, the operating turbine has a rated power of 1.2 MW at  $2.25 \text{ m s}^{-1}$ . This rated speed is similar to the reduced maximum free-stream flow in the example channel of  $2.3 \text{ m s}^{-1}$  with 680 turbines, where the 2.3 MW in Table 1 at the 89% overall efficiency of the operating turbine would give an output of 2.0 MW. Thus in a 680 turbine farm the operating turbine's 1.2 MW output as an isolated turbine could be boosted to 2.0 MW at the same flow velocity due to the additional power generated by head loss across the farm. Staggering turbines in adjacent rows [24] could further boost turbine output above 2.0 MW.

### 5.1. Turbine structural loads

Turbines in a single row farm in the example channel have a higher output than the first turbine installed in the channel, Fig. 3. This comes at a cost of higher structural loads, despite the reduction in free-stream flow due to power extraction by the farm. These higher loads are due to a transition, from generating power from

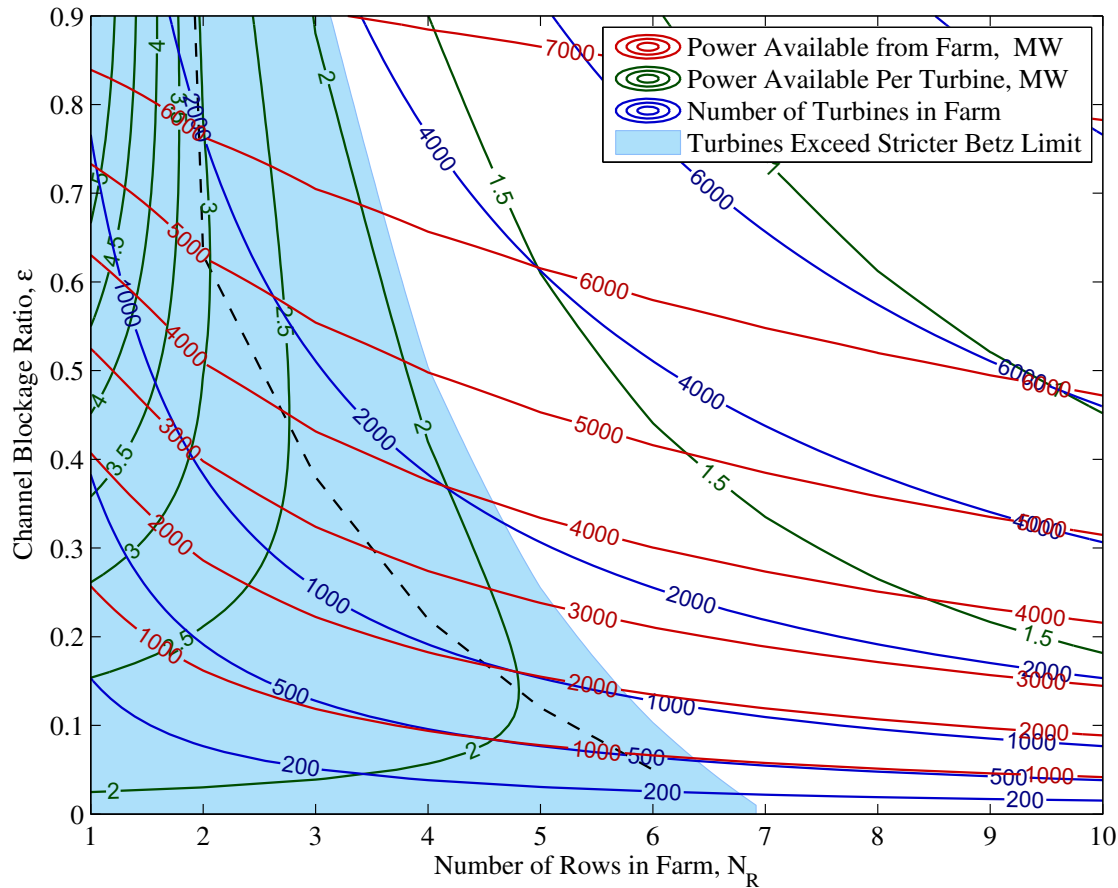


**Fig. 6.** Expanded version of Fig. 5 showing power for a range of farm configurations in a channel loosely based on the Pentland Firth at peak tidal flow. Red contours are the power available from the farm, green contours are the power available per turbine and blue contours the number of turbines in the farm. All shown farm configurations have  $C_p^{\text{opt}} > 16/27$  and light blue area shows those which also meet the stricter definition of exceeding the Betz limit (10). Also  $C_p^{1/3} \geq 16/27$  for all shown configurations. Configurations left of the black dashed line also have an increasing return on turbines added to the cross-section. (For interpretation of the references to color in this figure legend, the reader is referred to the web version of this article.)

momentum loss by the flow, to generating power from head loss across the row. Thus despite the turbines operating in lower flows they will need structurally stronger blades due to the pressure forces associated with the water level difference between upstream and downstream of the row. The turbine in a single row farm will also need stronger supporting structures and anchoring than that for an isolated turbine. Adding rows to a farm reduces the loads on the turbines, so that for  $\epsilon = 0.35$  in the example channel the power per turbine and the forces on the turbines within a 5 row farm are similar to those on an isolated turbine (Fig. 4h). Farms arranged to take advantage of turbines which meet the stricter definition of exceeding the Betz limit (10) will need a different design specification for the structural strength of their blades and support structures depending on the number of turbines and how they are arranged within the farm.

## 6. Conclusions

Like wind turbines, tidal turbines must be grouped together into farms with hundreds of turbines to make a significant contribution to the demand for renewable power. Tidal turbines within a farm in a high flow tidal channel can individually produce more power than an isolated single turbine, thus meeting a stricter definition of exceeding the Betz limit (10). However, exceeding this limit requires much more restrictive conditions than having turbines with a power coefficient  $C_p > 16/27$ . Consequently, laboratory or

numerical models which find  $C_p > 16/27$  at high blockage ratios for a fixed free-stream flow do not provide a complete picture of the conditions required to exceed the Betz limit, because they do not allow for the effects of flow reduction on maximum turbine output. Meeting the stricter definition of exceedance (10) is more difficult and will require a number of compromises and modifications to turbine design.

To significantly exceed the power output of the first Betz turbine requires a high channel blockage ratio, which may compromise navigation along the channel. Also, exceedance (10) requires farms to have a relatively small number of rows of turbines, which limits the maximum power the farm can produce, Fig. 6. Thus exceedance is a compromise between navigation, maximizing the power produced by each turbine and maximizing the total power produced by the farm. This compromise is illustrated in Fig. 6. Farms with a very small number of rows not only meet the stricter definition for exceedance, but may enjoy a second benefit, one where adding turbines to a row increases the output of all turbines in the farm. While exceedance is possible in the example channel given here, not all channels can have turbines which exceed the stricter Betz limit. For very small channels, e.g. 2 km long and 20 m deep, bottom friction dominates channel dynamics. For these small channels the turbines in a farm does not exceed the power output of the first turbine installed [11].

Exceedance (10) comes at a cost of higher structural loads on the turbine's blades, support structures and moorings, which will

require more robust turbine designs. These higher loads result from the head loss across a row of turbines which develops as the source of the turbine's power progressively changes as the farm grows, from momentum loss by the flow, to head loss across each row. Along with the higher loads, turbines will also need to be designed to operate in lower flows than that experienced by the first turbine installed in the channel due to the flow reduction which results from power extraction.

Turbines will also need the ability to be tuned for the particular channel and turbine arrangement to optimize turbine and farm output [10]. Adopting a fixed tuning which is the same tuning as that of the first turbine installed,  $r_3 = 1/3$ , produces less power from each turbine and results in higher structural loads than the optimal tuning of  $V_{10}$ . As turbines are added to a single row the higher loads of adopting a fixed tuning become significant before the lower power production of a fixed tuning becomes significant.

Much of the current effort in tidal current power centers on designing, manufacturing and deploying a single turbine, as a step towards developing arrays with less than 10 turbines. Ultimately arrays need 10s–100s of turbines to make a significant contribution to the demand for renewable power. On this scale turbines in farms perform very differently to single isolated turbines. In particular, turbines in a farm at maximum power output a) may have  $C_p \geq 16/27$  or  $C_p < 16/27$ , b) will experience a reduced maximum flow, c) may produce more or less power than an isolated turbine and, d) may experience higher or lower structural loads. Thus the way turbines are viewed and the criteria used to design them needs to change as we progress towards developing large arrays of tidal turbines.

## References

- [1] Betz A. Das Maximum der theoretisch möglichen Ausnutzung des Windes durch Windmotoren. *Gesamte Turbinenwesen* 1920;17:307–9.
- [2] Manwell J, McGowan J, Rogers A. *Wind energy explained*. Wiley Online Library; 2002.
- [3] Garrett C, Cummins P. The power potential of tidal currents in channels. *Proceedings of the Royal Society A* 2005;461:2563–72.
- [4] Vennell R. Tuning turbines in a tidal channel. *Journal of Fluid Mechanics* 2010; 663:253–67. <http://dx.doi.org/10.1017/S0022112010003502>.
- [5] Blunden LS, Bahaj AS. Tidal energy resource assessment for tidal stream generators. *Proceedings of the Institution of Mechanical Engineers, Part A: Journal of Power and Energy* 2007;221:137–46. <http://dx.doi.org/10.1243/09576509JPE332> (10).
- [6] Douglas C, Harrison G, Chick J. Life cycle assessment of the Seagen marine current turbine. *Proceedings of the Institution of Mechanical Engineers, Part M: Journal of Engineering for the Maritime Environment* 2008;222(1):1–12. <http://dx.doi.org/10.1243/14750902JEME94>.
- [7] Garrett C, Cummins P. The efficiency of a turbine in a tidal channel. *Journal of Fluid Mechanics* 2007;588:243–51.
- [8] MacLeod A, Barnes S, Rados K, Bryden I. Wake effects in tidal current turbine farms; 2002. p. 49–53.
- [9] Nishino T, Willden R. Effects of 3-D channel blockage and turbulent wake mixing on the limit of power extraction by tidal turbines. *Journal of Heat and Fluid Flow* 2012;37:123–35.
- [10] Vennell R. Tuning tidal turbines in-concert to maximise farm efficiency. *Journal of Fluid Mechanics* 2011;671:587–604. <http://dx.doi.org/10.1017/S0022112010006191>.
- [11] Vennell R. The energetics of large tidal turbine arrays. *Renewable Energy* 2012;48:210–9. <http://dx.doi.org/10.1016/j.renene.2012.04.018>.
- [12] Vennell R. Realizing the potential of tidal currents and the efficiency of turbine farms in a channel. *Renewable Energy* 2012;47:95–102. <http://dx.doi.org/10.1016/j.renene.2012.03.036>.
- [13] Corten G. Heat generation by a wind turbine. In: 14th IEA Symposium on the Aerodynamics of Wind Turbines, vol. ECN Report ECN-RX-01-001; 2000. p. 7.
- [14] Lanchester FW. A contribution to the theory of propulsion and the screw propeller. *Transactions of the Institution of Naval Architects LVII* 1915:98–116.
- [15] Vennell R. Observations of the phase of tidal currents along a strait. *Journal of Physical Oceanography* 1998;28(8):1570–7. [http://dx.doi.org/10.1175/1520-0485\(1998\)028<1570:OOTPOT>2.0.CO;2](http://dx.doi.org/10.1175/1520-0485(1998)028<1570:OOTPOT>2.0.CO;2).
- [16] Vennell R. Oscillating barotropic currents along short channels. *Journal of Physical Oceanography* 1998;28(8):1561–9. [http://dx.doi.org/10.1175/1520-0485\(1998\)028<1561:OBCASC>2.0.CO;2](http://dx.doi.org/10.1175/1520-0485(1998)028<1561:OBCASC>2.0.CO;2).
- [17] Bryden I, Couch S. ME1 marine energy extraction: tidal resource analysis. *Renewable Energy* 2006;31(2):133–9.
- [18] Baston S, Harris R. Modelling the hydrodynamic characteristics of tidal flow in the Pentland Firth. In: *Proceedings European Wave and Tidal Energy Conference* 2011, no. 317; 2011. p. 7.
- [19] Egbert G, Bennett A, Foreman M. Topex/poseidon tides estimated using a global inverse model. *Journal of Geophysical Research* 1994;99:24821–52.
- [20] Vennell R. Estimating the power potential of tidal currents and the impact of power extraction on flow speeds. *Renewable Energy* 2011;36:3558–65. <http://dx.doi.org/10.1016/j.renene.2011.05.011>.
- [21] McAdam R, Houlsby G, Oldfield M, McCulloch M. Experimental testing of the transverse horizontal axis water turbine. *Renewable Power Generation, IET* 2010;4(6):510–8.
- [22] Houlsby G, Draper S, Oldfield M, et al. Application of linear momentum actuator disc theory to open channel flow. Technical Report; 2008.
- [23] Whelan JI, Graham JMR, Peir J. A free-surface and blockage correction for tidal turbines. *Journal of Fluid Mechanics* 2009;624:281–91. <http://dx.doi.org/10.1017/S0022112009005916>.
- [24] Turnock S, Phillips A, Banks J, Nicholls-Lee R. Modelling tidal current turbine wakes using a coupled RANS-BEMT approach as a tool for analysing power capture of arrays of turbines. *Ocean Engineering*.